An Estimation Theoretic Approach to 3-D Image Interpolation

NELSON D. A. MASCARENHAS[1]
ILANA A. SOUZA[1]
PAULO E. CRUVINEL[2]
CLOVIS I. BISCEGLI[2]
REINALDO R. ROSA[3]
[1]Universidade Federal de São Carlos – Depto. de Computação C.P. 676 CEP 13565-905 São Carlos, SP, Brasil
{nelson, ilana}@dc.ufscar.br
[2]Empresa Brasileira de Pesquisa Agropecuária – Centro Nacional de Pesquisa e Desenvolvimento de Instrumentação Agropecuária C.P. 572 CEP 13560-970, São Carlos, SP, Brasil
{cruvinel,clovis}@cnpdia.embrapa.br
[3]Instituto Nacional de Pesquisas Espaciais – Laboratório Associado de Computação C.P. 515 CEP 12201-970 São José dos Campos, SP, Brasil
reinaldo@lac.inpe.br

Abstract. This paper presents a new approach to image 3-D interpolation using Bayesian estimation theory. Two methods are presented, depending on the used *a priori* information. The approach is applied to interpolate X-Ray images from the solar atmosphere taken at different depths, as well as RMN tomographic images of a tomato.

1. Introduction

In several applications, it is necessary to perform 3-D interpolation between 2-D sets of data, as a preliminary step for visualization, manipulation and analysis of 3-D scenes. In tomographic procedures, for example, one often needs to interpolate between 2-D slices. The objective of this paper is to develop new methods for 3-D interpolation based on Bayesian estimation theory.

In general, interpolation techniques can be divided into two categories [1],[2],[3]: scene-based and object-based interpolation. In the first case, the density values of the interpolated scene are directly determined from the density values of the given scene. In the second case, some information from an object extracted from the given scene is used to guide the interpolation process.

The simplest of the scene-based methods is the nearest-neighbor [4]. It assigns the pixel to the value of the nearest pixel. For 1-D problems, the linear interpolation between neighboring pixels is frequently used. For 2-D problems, the bilinear inepolation consists in first interpolating linearly along the rows of the image and then interpolating along the columns, or vice-versa. Although each operation is linear, the sequential application results in a surface which is non-linear [4]. Higher order polynomials, are often used. Cubic splines, B-splines, modified cubic splines are examples of these techniques. B-splines were used by Ribeiro and Cruvinel [5] to obtain intermediate planes in tomographic reconstruction. Modified cubic splines were examined in tomography by Herman et al [6]. Among the statistically based methods, one could mention the method of kriging, originally developed in Geostatistics [7]. Mascarenhas et al [8] and Zaniboni and Mascarenhas [9] developed a 2-D statistically based interpolation method as a preliminary step for image data fusion of multispectral images

The first object-based method was the shape-based interpolation method originally proposed by Raya and Udupa [10] for binary input scenes. The objective is to interpolate structures, instead of images, using their information, expressed in the form of distances to boundaries. This method was subsequently improved by Herman et al [11], who analysed several techniques based on the concept of chamfer distances. Goshtasby et al [12] proposed another object-based interpolation method, which was improved by Traina et al [13]. It consists of the application of two steps: a matching phase , which defines the corresponcence between points of each pair of images. For the second step, the latter

0-7695-0878-2/00 $10.00 © 2000 IEEE

authors used the Delaunay triangulation. Other methods for object–based interpolation were proposed by Chen et al [14] and Higgins et al[15]

Although object-based interpolation methods are able to obtain improved results, as compared to scene interpolation methods, they tend to be more computationally intensive. Our method could be considered a scene-based 3-D interpolation method, but the interpolation method depends statistically on the observed scenes and on an observed a priori intermediate image or on a statistical a priori model , if the first situation is not feasible.

2. Description of the Proposed Method

The objective of the method is to interpolate an intermediate image half-way between a pair of observed images. .The final objective would be to continue the procedure, by interpolating more planes and being able to perform a 3-D visualization process. However, the first interpolation contains all the features of the proposed method.

The pixels of the observed images are considered sets of observed random variables, Likewise, the pixels to be estimated on the interpolated image are also considered random variables. This framework is therefore based on a Bayesian approach for 3-D interpolation

The interpolation is locally based: pixel values on small neighborhoods on the top and bottom images are observed (3X3, 5X5 or 7X7) and the pixel located on the position corresponding to the center of those neighborhoods on the image to be interpolated is estimated, based on those values.

Under the Bayesian approach, it is necessary to have not only statistical infornation about the observations, but also the statistical dependence of the pixel random variables to be estimated on the observed pixel random variables over the two images (top and bottom) and a priori statistical information about the pixels to be interpolated.

Two different methods were used to provide this information: a) when sufficiently large observed images were available (see the remark below about the estimation problems that were faced) and an a priori image of the same size was also available for the interpolated image, then all the parameters of the estimation procedure were estimated; b) when the previous situation was not feasible, either because the observed images were not large enough, or because there was not an available a priori image for the interpolated image, then the a priori statistical information had to be partially postulated.

For method a), the statistical information about the observations is provided by the estimated expected values of each observed image, given by the sample mean over the whole image and by the covariance matrix C_{xx} of the observed values over the neighborhood, lexicographically ordered by columns, rows and images, estimated by its sample value over the whole observed images. The sample mean values are subtracted from the observed images and the sample mean of the estimated image is added at the end of the estimation process. The covariance matrix C_{xx} is 18X18 for a 3X3 neighborhood in each of the two observed images. For a 5X5 neighborhood, C_{xx} is 50X50 and, for 7X7, C_{xx} is 98X98. This increase on the size of the covariance matrix and the subsequent dimensionality of the parameter estimation problem demands an increase on the amount of observed data [16]. We were able to use the version of the method that depends on the estimation of the covariance matrix C_{xx} only for the smallest neighborhood (3X3) and the largest available observed images (256X256). For smaller images and/or larger neighborhoods, the estimates of C_{xx} displayed negative or complex conjugate eigenvalues, precluding the estimation of C_{xx} to be a valid positive –definite covariance matrix.

The statistical information about the dependence of the random variable that describes the central pixel to be estimated on the observed random variables over the local neighborhoods on the two images is obtained by the sample covariances (18 for a 3X3 neighborhood, for example) obtained over the whole images.

The statistical a priori information about the image to be estimated was obtained through the sample mean and sample variance over the whole a priori available image.

For method b) we had to postulate several statistical parameters, instead of estimating them. The sample mean values, the sample variance values of the observed images, as well as the sample covariance value between corresponding pixels in the two observed images could be obtained. However, the covariance between other

observed random variables in the two images had to be defined. We adopted a covariance estructure that was separable in the spatial and the spectral domains. Spatial correlation coefficients of .95 in the vertical and horizontal directions were chosen, as often done in the literature.

The dependence between the random variable to be estimated and the observed values was chosen according to the folowing procedure: the covariance structure was suposed to be separable in the spatial and the vertical domains. The 2-D correlation coefficients on the horizontal and the vertical domains were selected to be either .95 or 1.0. In this last case, we postulated that all observed random variables over the window had the same correlation with the random variable to be estimated. The 3-D correlation coefficient between the estimated pixel and the corresponding pixels on the observed images was selected to be the square root of the estimated correlation coefficient between the observed images (for the cases that we observed, this value was positive, when estimated over the whole images)

The a priori information about the interpolated image with method b) was specified by the mean value of the image (assumed to be the arithmetic mean of the sample mean values of the observed images) and the variance, asumed to be the geometric mean of the variances of the observed images

Observe that even if the observed images do not provide enough sample values for the estimation of the large number of parameters of the covariance matrix C_{XX}, it is still possible to estimate other parameters like covariances between the estimated pixel and the observed pixels, expected value and variance of the a priori image, if this image is available This procedure would reduce the amount of hypotheses that have to be made about the statistical model. However, for this work the interpolation was performed according to methods a) and b) only. For the next future, we are planning to generate interpolated images, by using the estimation procedures described in this paragraph and compare them with the images generated by methods a) and b)

3. The Linear Mean Square Interpolator

We adopted the mean square error as a criterion to derive the local interpolator. It is a well known result in estimation theory that, if the estimator is constrained to be linear, the mean square error is minimized by applying the orthogonality principle [17].

Let $\mathbf{X}$ denote the column vector of observed random variables over the two neighborhoods on the top and bottom images. For example, for 3X3 neighborhoods, the dimension of $\mathbf{X}$ will be 18. Assume that we have already removed the mean values of the observed images. Therefore, we can consider that $\mathbf{X}$ is a zero mean random vector. Denote by Y the scalar random variable to be estimated on the interpolated image, on the center of the neighborhood. According to the orthogonality principle, the LMMSE (linear minimum mean square error) estimator for Y based on the observed vector $\mathbf{X}$ is given by:

$$Y=a^T\mathbf{X}$$

where

$$a^T = k_{YX}.(K_{XX})^{-1}$$

$$k_{YX} = E[Y\mathbf{X}^T]$$

and

$$K_{XX} = E[\mathbf{X}\mathbf{X}^T]$$

The values for k_{YX} and K_{XX} are obtained in different ways, depending on whether we are using method a) or b), as was explained previously. If we use method a), then the expected values are estimated by the sample values over the whole observed images.

The resulting scalar random variable Y has zero mean. To complete the estimation process, we have to add to the estimated Y its mean value.

The resulting mean square error is obtained by:

$$MSE = var(Y) - k_{YX}.(K_{XX})^{-1}(k_{YX})^T$$

The reduction of the MSE from the variance of Y is due to the correlation that exists between the observed vector $\mathbf{X}$ and the random variable to be estimated Y.

4. Interpolation of the Solar Images

The X-Ray images of the solar atmosphere were obtained by the Japanese satellite Yohkoh, launched on August 30th, 1991, with the objective to follow the solar atmosphere explosions, which are the cause of serious perturbations on terrestrial communications. We used a set of two 128X128

images at two different depths on the solar atmosphere, without any intermediate image, that could serve as a priori image on the interpolation process. The size of the images were not enough to get positive definite estimates of the correlation matrix K_{XX}, even for the smallest window (3X3). Therefore, we used method b) for the interpolation process.

The observed images are displayed below.

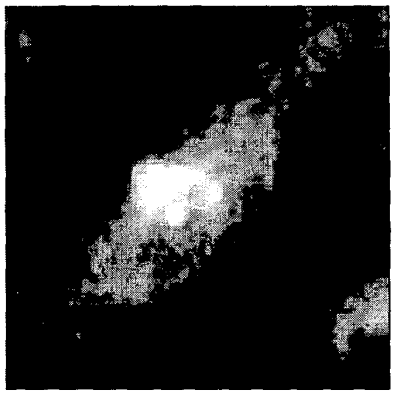

Figure 1 – Solar Image A
Sample Mean Value of A: 43.00

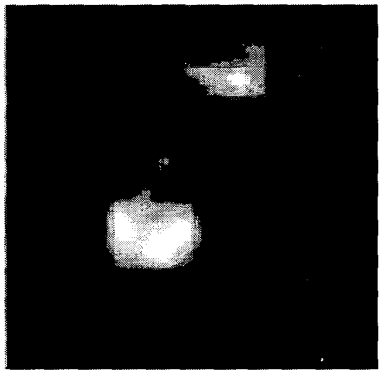

Figure 2 – Solar Image B
Sample MeanValue of B: 39.17

The interpolated images using method b), with spatial correlation coefficients .95 and 1.0 , as described above, are displayed below:

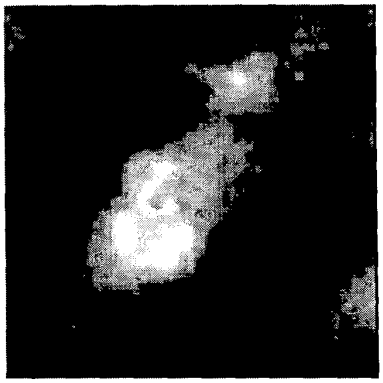

Figure 3–Interpolated Solar Image:ρ =0.95
Sample Mean Value of Figure 3: 41.25
A Priori Mean Value: 41.09
Theoretical MSE: 648.22
A Priori Variance: 1360.0

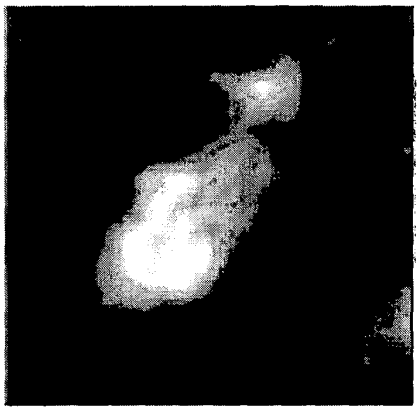

Figure 4 – Interpolated Solar Image: ρ = 1.0
Sample Mean Value of Figure 4: 41.27
A Priori Mean Value: 41.09
Theoretical MSE: 573.34
A Priori Variance: 1360.0

5. Interpolation of Magnetic Resonance Images

The NMR agricultural images were obtained by means of a 2T super conducting magnet from Varian, model Inova 400MHz. Two images of tomatoes, both with 256X256 pixels and resolution of 1 mm^2 were taken using a spin-echo based pulse sequence. Pulse sequence parameters were 15ms TE (Time of Echo), 200 ms TR (Time of Repetition) and approximately 100mm field of

view (FOV) in x and y direction. The observed images are displayed below.

Figure 5 – Top RMN Image of the Tomato (A)
Sample Mean Value of A: 49.18

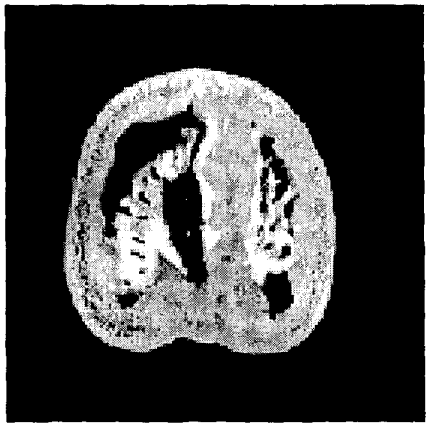

Figure 6: Bottom RMN Image of the Tomato (B)
Sample Mean Value of B: 53.34

When an a priori intermediate image was used (see Figure 7 below), we used method a), with a 3X3 neighborhood. As stated above, larger neighborhoods did not allow a satisfactory estimation of the covariance matrix C_{xx}

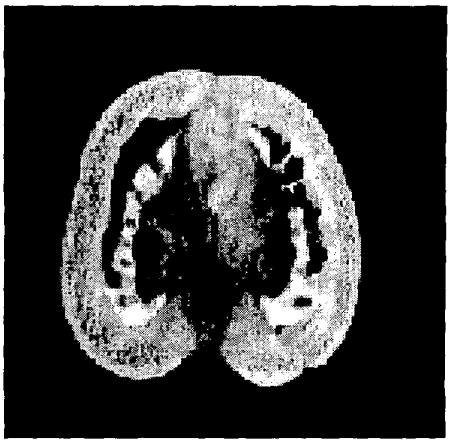

Figure 7 – Intermediate a priori Image
Sample Mean Value of Figure 7: 49.78
Sample Variance of Figure 7: 5737.8

Figure 8 below displays the result of the application of method a), with a 3X3 neighborhood

Figure 8 – Interpolated Image (method a) – 3X3 neighborhood
Sample Mean of Figure 8: 50.53
A Priori Mean Value: 49.78
Theoretical MSE: 1432.3
Experimental MSE: 1522.9
A Priori Variance: 5737.8

The experimental MSE was calculated by taking the sample mean value of the square error between the intermediate a priori image and the interpolated image.

When no intermediate a priori image was used, then method b) was chosen and the results for $\rho = .95$ and 1.0 are displayed below, in Figures 9 and 10, respectively.

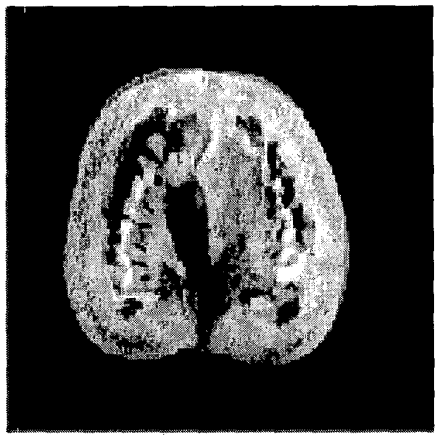

Figure 9 – Interpol. Image (method b) – $\rho = .95$
Sample Mean Value of Figure 9: 52.06
A Priori Mean Value: 51.26
Theoretical MSE: 936.38
A Priori Variance: 5764,1

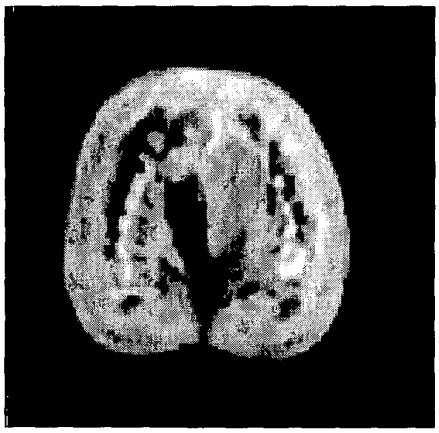

Figure 10 – Interpol. Image (method b) - $\rho = 1.0$
Sample Mean of Figure 10: 52.14
A Priori Mean Value: 51.26
Theoretical MSE: 428.54
A Priori Variance: 5764,1

6. Conclusions

The visual results presented by the interpolated images are reasonable: with method a) (tomato image), the interpolated image is a blend of the a priori intermediate image and the observed top and bottom images; with method b) (solar and tomato images), the interpolated image is a blend of the observed top and bottom images.

With method b), the images interpolated with $\rho = .95$ are sharper than with $\rho = 1.0$, for both images.

From the quantitative point of view, the results are also coherent: 1) the sample mean values of the interpolated images are close to the a priori mean values; 2) the theoretical MSE are lower than the a priori variance; 3) the experimental MSE in method a) is lower than the a priori variance and somewhat higher than the theoretical MSE.

We intend to continue the work by interpolating more images between the top and bottom ones , in order to perform a 3-D visualization of the data structure. Also, we plan to develop the hybrid method of estimation, when there is not enough data to estimate the covariance matrix of the observations, but an intermediate a priori image is available. Further investigation on the covariance estimation procedure with limited sample data would be useful in our problem. We are also studying methods to cope with discontinuities between blocks of data with spatially adaptive interpolation methods.

7. Acknowlegements

The authors want to acknowlege the support of FINEP-RECOPE Project # 77.97.0575.00 and FINEP-FNDCT Project # 77.97.0452.00. The work of Miss Ilana A. Souza was supported by a CAPES scholarship.

8. References

[1] G. J. Grevera, J. K. Udupa, "Shape-based interpolation of multidimensional grey-level images", *IEEE Transactions on Medical Imaging*, Vol. 15, No. 6, December 1996, pp. 881-892.

[2] G. J. Grevera, J. K. Udupa, "An objective comparison of 3-D image interpolation methods", *IEEE Transactions on Medical Imaging*, Vol. 17, No. 4, August 1998, pp. 642-652.

[3] G. J. Grevera, J. K. Udupa, " A task-specific evaluation of three-dimensional image interpolation techniques", *IEEE Transactions on Medical Imaging,*, Vol. 18, No. 2, February 1999, pp. 137-143.

[4] W. K. Pratt, *"Digital image processing"*, Wiley, 2nd. Ed., 1991.

[5] G. C. Ribeiro, P. E. Cruvinel, "Tridimensional image reconstruction method based on the modified algebraic reconstruction technique and B-spline interpolation", *Anais do X SIBGRAPI,* 1997, pp. 111-118.
[6] G. T. Herman, S. W. Rowland, M.-M. Yau, "A Comparative study of the use of linear and modified cubic spline interpolation for image reconstruction", *IEEE Transactions on Nuclear Science,* vol. NS-26, No. 2, April 1979, pp. 2879-2894.
[7] M. R. Stytz, R. W. Parrott, "Using kriging for for 3-D medical imaging", *Computerized Med. Imag. Graphics,* Vol. 17, No. 6, 1993, pp. 421-442.
[8] N. D. A. Mascarenhas, Banon. G. J. F, Candeias, A. L. B., "Multispectral image data fusion under a bayesian approach", *International Journal of Remote Sensing,* Vol. 17, No. 8, 1996, pp. 1457-1471.
[9] G. T. Zaniboni, N. D. A. Mascarenhas, "Fusão bayesiana usando coeficientes de correlação localmente adaptáveis", *Anais do VIII Simpósio Brasileiro de Sensoriamento Remoto,* !998, Electronic Publication in CD-ROM, File: 8_135o.pdf.
[10] S. P.Raya, J. K. Udupa, "Shape-based interpolation of multidimensional objects", *IEEE Tansactions on Medical Imaging,* Vol. 9, No. 1, March 1990, pp. 32-42.
[11] G. T. Herman, J. Zheng, C. A. Bucholtz, "Shape-based interpolation", *IEEE Computer Graphics & Applications,* May 1992, pp. 69-79.
[12] A. Goshtasby, D. A. Turner, L. V, Ackerman, "Matching of tomographic slices for interpolation", *IEEE Transactions on Medical Imaging,* Vol. 11, No. 4, December 1992, pp. 507-516.
[13] A. J. M. Traina, A. J. M. A. Prado, J. M. Bueno, "3D reconstruction of tomographic images applied to largely spaced slices", *Journal of Medical Systems,* Vol. 21, No. 6, December 1997, *pp. 353-367.*
[14] S. Y. Chen, W. C. Lin, C. C. Liang, C. T. Chen, "Improvement on dynamic elastic interpolation technique for reconstructing 3-D objects from serial cross sections", *IEEE Transactions on Medical* Imaging, Vol. 9, No. 1, March 1990, pp. 71-83.
[15] W. E. Higgins, C. Morice, E. L. Ritman, "Shape-based interpolation of tree-like structures in three-dimensional images", *IEEE Transactions on Medical Imaging,* Vol. 12, No. 3, September 1993, pp. 439-450.
[16] S. Tadjudin, D. A. Landgrebe, "Covariance estimation with limited training samples", *IEEE Transactions on Geoscience and Remote Sensing,* vol. 37, No. 4, July 1999, pp. 2113-2118.
[17] H. Stark, J. W. Woods, *"Probability, random processes and estimation theory for engineers"* , Prentice Hall, 2nd Ed.., 1996.